Akademeia (2012) 2(1): ea0114

Applied Sciences
ARTICLE

Static and dynamic characteristics of an inverted three-lobe pressure dam bearing

Neel Kamal Batra[1], Gian Bhushan[2] and N.P. Mehta[1] ‡

[1] *Maharishi Markendeshwar Engineering College, Ambala (Haryana), India*

[2] *National Institute of Technology, Kurukshetra (Haryana), India*

The stability of journal bearings is found to be increased by the use of multilobes. Studies have shown that performance is further increased by the use of pressure dams. This paper analyses the performance of an inverted three-lobe pressure dam bearing, which is produced by incorporating a pressure dam in the upper lobe and two relief tracks in the lower two lobes of an ordinary inverted three-lobe bearing. A generalized Reynolds equation has been derived for carrying out the stability analysis of an inverted three-lobe pressure dam bearing that has been solved using the finite element method. The results indicate that the performance of an inverted three-lobe pressure dam bearing is better than an ordinary three lobe pressure dam bearing.

KEYWORDS: Inverted three-lobe pressure dam bearing, finite element method, ellipticity ratio

The enormous progress of modern engines and machinery has required the development of bearings operating under higher speed and pressures. It has been observed that the performance of ordinary circular bearings is not satisfactory at high speeds [1]. Several papers are available which deal with performance enhancement from manipulating geometrical changes of the journal bearing system and the lubricating fluid [2,3]. However, to increase the stability of ordinary journal bearings the use of multi-lobes and the incorporation of pressure dams is preferred [5]. Dynamic analysis has shown cylindrical pressure dam bearings are very stable [6-9]. There are also non–cylindrical pressure dam such as finite– elliptical, half-elliptical, offset-halves, three–lobe and four-lobe [10-14]. According to Malik *et al.* [15]the performance of an inverted three-lobe bearing is better than that of a three-lobe bearing. As incorporation of pressure dams has proved to be useful in improving the stability of multilobe bearings, an inverted three lobe pressure dam bearing is expected to be more stable than an ordinary inverted three lobe bearing . Therefore the present study is undertaken to investigate the performance of an inverted three-lobe pressure dam bearing.

Bearing Geometry

Figure 1 shows the geometry of an inverted three-lobe pressure dam bearing. A rectangular dam or step of depth S_d and width L_d is cut circumferentially in lobe 1 of the bearing. Circumferential relief tracks or grooves of certain depth and width L_t are also cut centrally in lobes 2 and 3 of the bearing. Lobe 1 with pressure dam and lobes 2 and 3 with relief tracks are shown in **figure 2**. **Figure 3** shows Lobe 1 with pressure dam and lobes 2 and 3 with relief tracks. The relief tracks are assumed to be so deep that their hydrodynamic effects can be neglected. For a concentric position of the rotor, there are two reference clearances of the

‡Correspondence: nkbatraeng@rediffmail.com
Received: 30 September, 2011; **Accepted:** 29 March, 2012

bearing: a major clearance c given by a circle circumscribed by the lobe radius and a minor clearance c_m given by an inscribed circle. Thus, the centre of each lobe is shifted by a distance e_p=c-c_m, known as the ellipticity of the bearing. The various eccentricities and ellipticities are non-dimensionalized by dividing by the major clearance c.

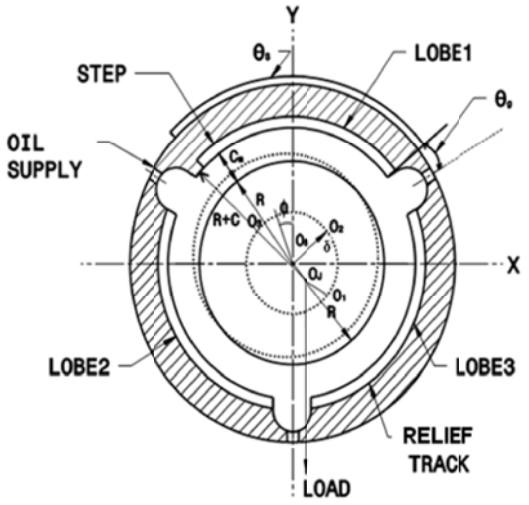

Figure 1. An inverted three-lobe pressure dam bearing

Ellipticity ratio is defined as:

$$(\delta) = (c - c_m)/c = 1 - c_m/c$$

Eccentricity ratio is defined as:

$$(\varepsilon) = e/c$$
$$\varepsilon_1 = e_1/c, \varepsilon_2 = e_2/c, \varepsilon_3 = e_3/c$$

If I_1 and I_2 are circumferential lengths of the bearing before and after the dam, then:

$$l_1 = \pi R\theta_s/180$$
$$l_2 = \pi R(120 - \theta_s - 2\theta_g)/180$$

The various eccentricity ratios and attitude angles of the lobes of an inverted three-lobe pressure dam bearing are given by:

$$\varepsilon_1^{\,2} = \varepsilon^2 + \delta^2 - 2\varepsilon\delta\cos\phi$$
$$\varepsilon_2^{\,2} = \varepsilon^2 + \delta^2 - 2\varepsilon\delta\cos(2\pi/3 - \phi)$$
$$\varepsilon_3^{\,2} = \varepsilon^2 + \delta^2 - 2\varepsilon\delta\cos(2\pi/3 + \phi)$$

$$\phi_1 = \pi - \sin^{-1}(\varepsilon\sin\phi)/\varepsilon_1)$$
$$\phi_2 = 5\pi/3 + \sin^{-1}(\varepsilon(\sin 2\pi/3 - \phi)/\varepsilon_2)$$
$$\phi_3 = \pi/3 - \sin^{-1}(\varepsilon(\sin 2\pi/3 + \phi)/\varepsilon_3)$$

Analysis

The Reynolds Equation for the laminar flow is:

$$\frac{\partial}{\partial x}\left(\frac{h^3}{\mu}\frac{\partial p}{\partial x}\right) + \frac{\partial}{\partial z}\left(\frac{h^3}{\mu}\frac{\partial p}{\partial z}\right) = 6R\omega\frac{\partial h}{\partial x} + +12\varepsilon\dot{\phi}\sin\theta + 12\dot{e}\cos\theta \quad (1)$$

This equation is non-dimensionalized by making the following substitutions:

$$\theta = \frac{x}{R} = \frac{2x}{D} = 2\bar{x},\ \varepsilon = \frac{e}{c},\ \dot{\alpha} = \frac{\dot{\phi}}{\omega}\ and\ \dot{\beta} = \frac{\varepsilon}{\dot{\omega}}$$
$$\bar{x} = \frac{x}{D},\ \bar{z} = \frac{z}{L},\ \bar{h} = \frac{h}{2c},\ \bar{p} = \frac{2\pi p}{\mu\omega}\left(\frac{c}{R}\right)^2$$

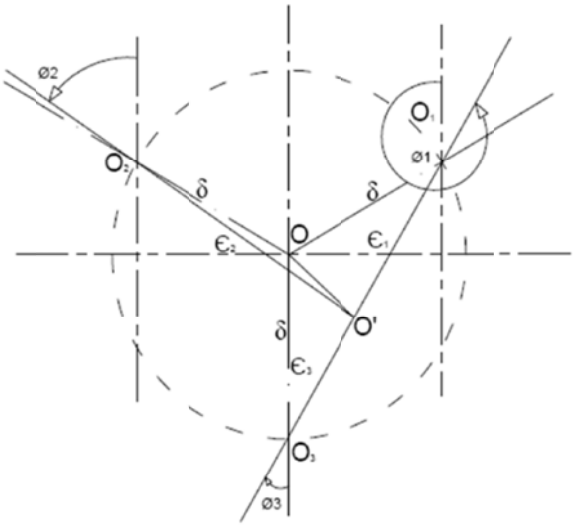

Figure 2. Diagram showing various attitude angles and eccentricity ratio

The non- dimensionalized equation thus obtained is:

$$\frac{\partial}{\partial\bar{x}}\left(\frac{\bar{h}^3}{12}\frac{\partial\bar{p}}{\partial\bar{x}}\right) + \left(\frac{D}{L}\right)^2\frac{\partial}{\partial\bar{z}}\left(\frac{\bar{h}^3}{12}\frac{\partial\bar{p}}{\partial\bar{z}}\right) = \frac{\pi}{2}\frac{\partial\bar{h}}{\partial\bar{x}} + \pi\varepsilon\dot{\alpha}\sin 2\bar{x} + \pi\dot{\beta}\cos 2\bar{x} \quad (2)$$

The various assumptions made in deriving the Reynolds Equation are that the fluid is Newtonian, no slip occurs at the bearing surface, inertia terms are neglected, oil viscosity is constant, and curvature is negligible. The Reynolds equation is analyzed for a pressure profile using the finite

element method. The solution of this equation is obtained by minimizing the following variation integral [18] over the individual elements:

$$J_e(\bar{p}_e)=\iint_{A_e}\left[-\frac{1}{2}\frac{\bar{h}^3}{12}\left\{\left(\frac{\partial \bar{p}_e}{\partial \bar{x}}\right)^2+\left(\frac{D}{L}\right)^2\left(\frac{\partial \bar{p}_e}{\partial \bar{z}}\right)^2\right\}+\frac{\pi}{2}\bar{h}\frac{\partial \bar{p}_e}{\partial \bar{x}}-\frac{\pi}{2}\varepsilon\dot{\alpha}\cos 2\bar{x}\frac{\partial \bar{p}_e}{\partial \bar{x}}+\frac{\pi}{2}\dot{\beta}\sin 2\bar{x}\frac{\partial \bar{p}_e}{\partial \bar{x}}\right]dA_e \quad (3)$$

where $\bar{p}_e$ = dimensionless film pressure in the e[th] element.

The Reynolds equation is an elliptical partial differential equation and hence must be solved as a boundary-value problem. According to McCallion *et al.* [19] for a bearing having oil supplied at zero pressure, the largest possible extent of positive pressure region is given by the boundary conditions that both pressure and pressure gradient are zero at the breakdown and build up boundaries of the oil film. However, it has been shown [20] that even by setting the negative hydrodynamic pressure to zero as they occur in any iteration step, the results tends to satisfy the above mentioned boundary conditions in the limit. The latter approach has been followed in the present analysis. Stiffness and damping coefficients are determined separately for each lobe and then added. The values of these stiffness and damping coefficients, shaft flexibility, and

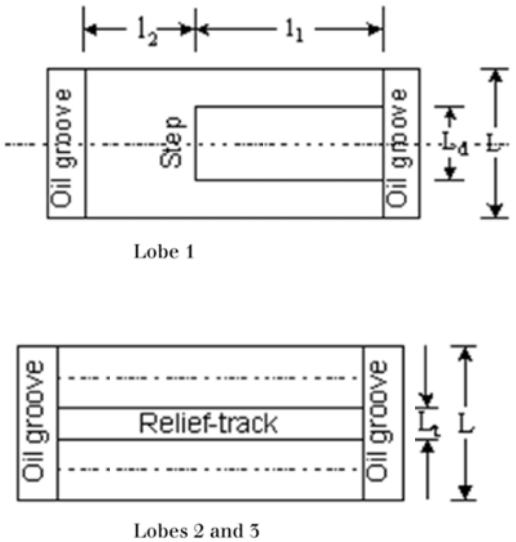

Figure 3. Lobes of an inverted three-lobe pressure dam bearing

dimensionless speed are then used to evaluate the coefficients of the characteristic equation [21],which is a polynomial of the 6[th] order for flexible rotors as given below (for a rigid rotor, F=0). This characteristic equation is given by:

$$s^6F^2v^4C_0+s^5v^4\left(F^2C_1+FC_2\right)+s^4v^2\left(v^2F^2C_3+2FC_0+v^2+v^2FC_4\right)+$$
$$s^3v^2\left(2FC_1+C_2\right)+s^2\left(2Fv^3C_3+v^2C_4+C_0\right)+sC_1+C_3=0$$

where

$$C_0=\bar{C}_{xx}\bar{C}_{yy}-\bar{C}_{xy}\bar{C}_{yx}$$
$$C1=\bar{K}_{xx}\bar{C}_{yy}+\bar{K}_{yy}\bar{C}_{xx}-\bar{K}_{xy}\bar{C}_{yx}-\bar{K}_{yx}\bar{C}_{xy}$$
$$C_2=\bar{C}_{xx}+\bar{C}_{yy}$$
$$C_3=\bar{K}_{xx}\bar{K}_{yy}-\bar{K}_{xy}\bar{K}_{yx}$$
$$C_4=\bar{K}_{xx}+\bar{K}_{yy}$$

For a rigid rotor, the value of F (dimensionless flexibility) is taken as zero. The system is considered as stable if the real part of all roots is negative. For a particular bearing geometry and eccentricity ratio, the values of dimensionless speed are increased until the system becomes unstable.

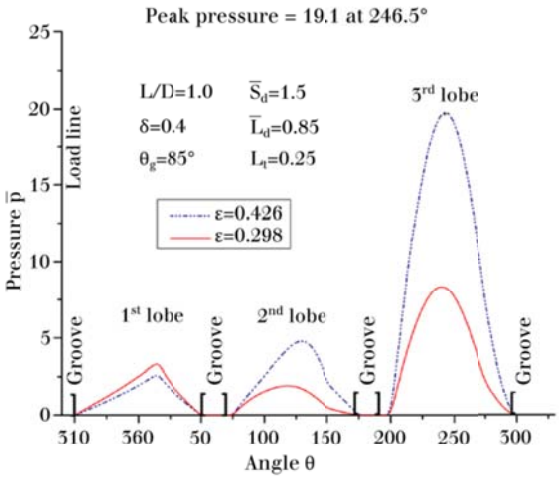

Figure 4. Maximum pressure variation over each lobe of the inverted three-lobe pressure dam bearing (δ=0.4)

The maximum value of speed for which the bearing is stable is then adopted as the dimensionless threshold speed. The stability threshold curves divide any figure into two major zones. The zone above this curve is unstable, whereas the zone below is stable. The minimum value of this curve is termed as the minimum threshold speed. Mostly, the curve has a vertical line, towards the left side of which the bearing is stable at all speed. This portion is called the zone of infinite stability.

The present analysis has been done for the bearing with the following parameters:

$L/D=1.0,\ \bar{S}_d=1.5,\quad \bar{L}_d=0.8,$
$\bar{L}_t=0.25,\quad \theta_s=85^\circ,\quad \theta_g=10^\circ$

Three values of ellipticity ratio (δ) = 0.4, 0.5, and 0.6, were selected for present study.

Results and Discussion

Figures 4 to 6 shows the circumferential variation of fluid film pressure at the centered line of an inverted three lobe pressure dam bearing for the values of ellipticity ratios (δ) 0.4, 0.5 and 0.6 respectively. The

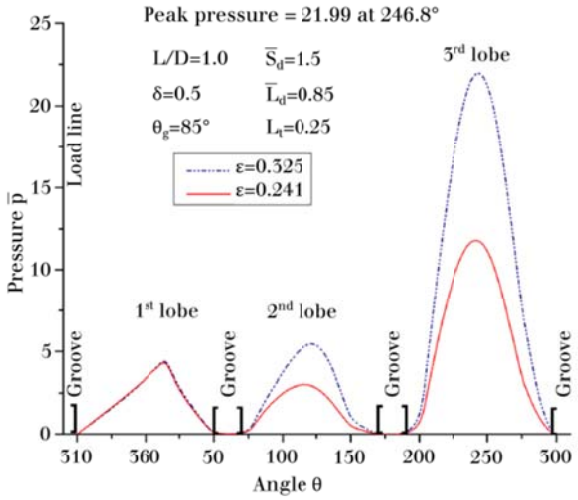

Figure 5. Maximum pressure variation over each lobe of the inverted three-lobe pressure dam bearing (δ=0.5)

circumferential angle in these figures is taken from the load line in the direction of rotation. The oil supply grooves are marked in each figure. In general, two extreme eccentricity ratios from the investigated range are taken for which centre- line pressures are plotted. Thus these plots show the limits of fluid film pressure in each lobe for a given set of design parameters in the investigation stage.
It is observed from these three plots (for δ = 0.4, 0.5, and 0.6) that the upper lobe (lobe1) is saturated with moderate to heavy pressures. **Figure 7** depicts the pressure in the three lobes of an ordinary inverted three lobe bearing at δ=0.5. The value of δ=0.5 is selected for comparison purpose as most of the researchers have taken this value. The figure shows that the lobe 1 is cavitated over most of the surface or

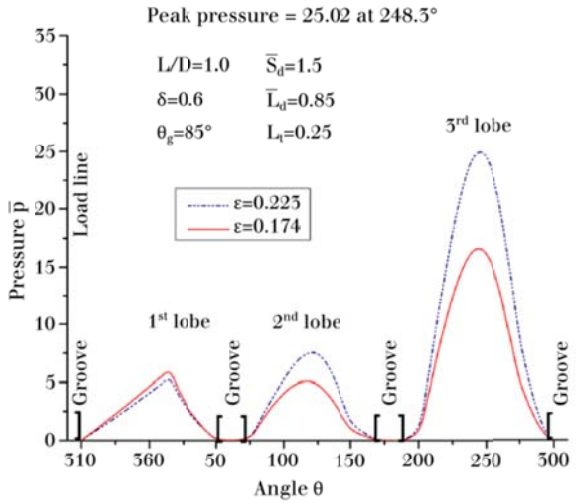

Figure 6. Maximum pressure variation over each lobe of the inverted three-lobe pressure dam bearing (δ=0.6)

has very low pressure. In the second and third lobes heavy pressure are usually developed on larger surfaces in all the cases. Thus, a comparison shows that an inverted three lobe pressure dam bearing would be very stiff as compared to an ordinary inverted three lobe bearing, indicating more stable operation.

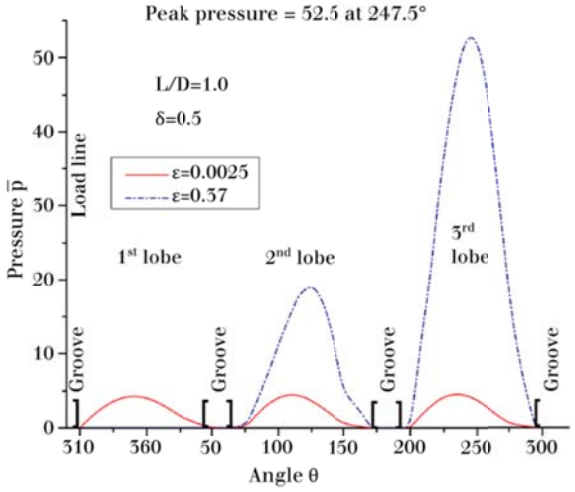

Figure 7. Maximum pressure variation over each lobe of an inverted three-lobe bearing (δ=0.5)

Figure 8 shows the variation of minimum film thickness with Sommerfeld number for an inverted three–lobe pressure dam bearing (for δ= 0.4, 0.5, and 0.6) and an ordinary three lobe pressure dam bearing (for δ= 0.5). Minimum film thickness is calculated from the expression:

hmin = c(1- larger value of the lobe eccentricity ratios ε1, ε2, ε3 and ε4)

hmin is non-dimensionalized as:

$\bar{h}_{min}$ =hmin/c

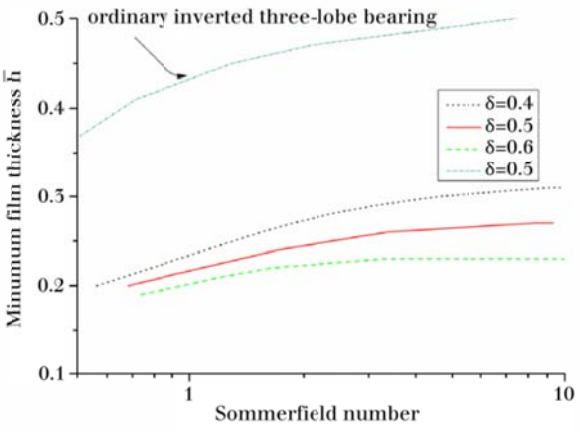

Figure 8. Sommerfield number versus minimum film thickness

This figure depicts that for a particular value of S, minimum film thickness decreases as the value of δ increases. It is also observed from the comparison of the curves for an ordinary inverted three lobe pressure dam bearing and inverted three-lobe pressure dam bearing that by incorporation of pressure dam, the minimum film thickness of the inverted three-lobe pressure dam decreases. **Figure 9** shows curves of friction coefficients versus Sommerfeld numbers for δ= 0.4, 0.5, and 0.6. There is no significant variation in friction with change in the value of ellipticity ratio. In general friction is observed to increase with an increase in sommerfeld number for all the values of δ.

The variation of dimensionless oil-flow coefficient with Sommerfeld number is shown in **figure 10**. This coefficient is calculated from the following expression [15]:

$$\bar{q} = \frac{1}{3\pi}\left(\frac{D}{L}\right)^2 \sum h^{-3} \frac{d\bar{p}}{d\bar{z}} \Delta\bar{x}$$

Where $\frac{d\bar{p}}{d\bar{z}}$

is the slope of pressure curves at the sides of bearing. From the figure it is observed that oil flow coefficient decreases with an increase in the value of δ for a

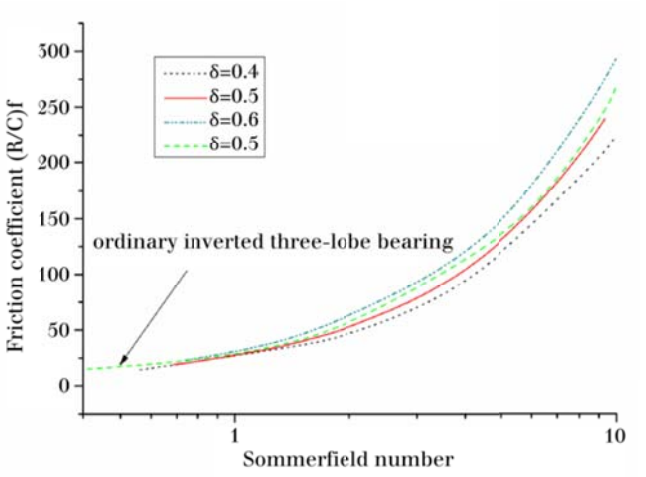

Figure 9. Sommerfield number versus friction coefficient

particular value of S.

A dimensionless friction coefficient (R/c) f, of a journal bearing is given by:

$$\left(\frac{R}{c}\right) f = \left[\int_0^1 \int_{\theta 1}^{\theta 2} \frac{\bar{h}}{2} \frac{\partial \bar{p}}{\partial \bar{x}} d\bar{x} d\bar{z} + \int_0^1 \int_{\theta 1}^{\theta 2} \frac{\pi}{\bar{h}} d\bar{x} d\bar{z} + \int_0^1 \int_{\theta 2}^{\theta 3} \frac{\pi \bar{h} 2}{\bar{h}^2} d\bar{x} d\bar{z}\right] \times S$$

Where h2 is the film thickness corresponding to δ.

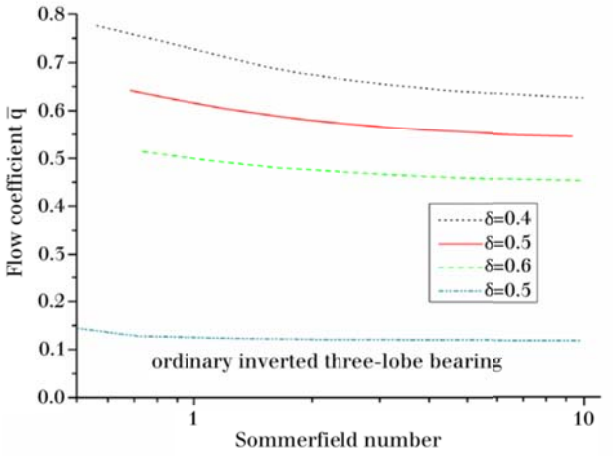

Figure 10. Sommerfield number versus flow coefficient

Figure 11 shows a comparison of dimensionless threshold speed with the variation of sommerfeld number for a ordinary three lobe bearing, inverted three lobe bearing and inverted three lobe bearing with pressure dam. All the curves are drawn for δ =0.5 and F=0. The curves show that in comparison with an ordinary inverted three-lobe bearing, the zone of infinite stability for the inverted three-lobe pressure dam bearing increases from S=0.09 to S=0.69. The minimum threshold speed is also found to increase from 6.05 to 16.5. The curve also indicates that there is a marginal decrease in the

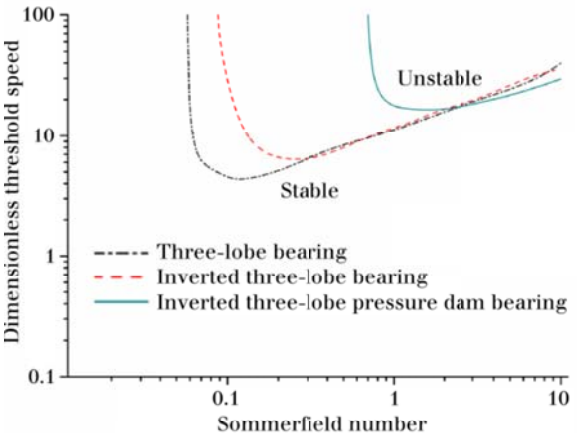

Figure 11. Comparison of stability characteristics of a three-lobe and inverted three-lobe bearing with and without a pressure dam

stability of inverted three-lobe pressure dam bearing for sommerfeld number more than 2.54. Thus, in general, the stability of an inverted three-lobe pressure dam bearing is better than an ordinary inverted three-lobe bearing.

Conclusion

1. The generation of pressure and their circumferential variation in the upper half of the bearing primarily affects the stability of a rotor bearing system. The proportion of the hydrodynamic load generated in the upper half of the bearing with respect to load generated in the lower half is one of the deciding factors of the bearing's stability. Thus higher pressure prevailing in a wider portion of the upper half of the bearing would have a positive effect on the stability of the bearing. In comparison with ordinary three lobes bearing the pressure in lobe1 of an inverted three lobe pressure dam bearing increases from 3.78 to 4.6, whereas, the pressure in the relief track decreases from 52.5 to 21.99, predicts the increase in the stability of the bearing.

As pressure generated in lobe 1 of an inverted three lobe pressure dam bearing is high as compared to lobe 1 of an ordinary inverted three lobe bearing, makes the inverted three lobe pressure dam bearing stiffer than an ordinary three lobe bearing. Therefore more stable operation is expected from an inverted three lobe pressure dam bearing as compared to an ordinary inverted three lobe bearing.

2. The values of oil minimum film thickness coefficients decreases where as the value of friction coefficient increases with increase in δ for a particular value of Sommerfeld number.

3. As the Sommerfeld number increases from 0.09 to 0.69, the curve shift towards the right side and thus the zone of stability increases. Even the minimum threshold speed increased from 6.05 to 16.5, making operation more stable.

Notation

c : Radial clearance

c_m : Minimum film thickness for a centered shaft

$C_{xx}, C_{xy}, C_{yx}, C_{yy}$: Oil - film damping coefficients

$\bar{C}_{xx}, \bar{C}_{xy}, \bar{C}_{yx}, \bar{C}_{yy}$: Dimensionless oil-film coefficients $\bar{C}_{xx} = C_{xx}(\omega c / W)$

C_0, C_1, C_2, C_3, C_4 : Coefficients of the characteristic equation

D : Diameter

e : Eccentricity

F : Dimensionless shaft flexibility, W/ck

h : Oil-film thickness, $c(1+\varepsilon\cos\theta)$

$\bar{h}$: Dimensionless oil-film thickness, h/2c

$\overline{L_d}$: Non-dimensionalized relief track width L_d/L

$\overline{L_t}$: Non-dimensionalized relief track width L_t/L

$\overline{S_d}$: Non-dimensionalized relief track width S_d/c

$\bar{q}$: Dimensionless oil flow coefficient.

$2k$: Shaft stiffness

$K_{xx}, K_{xy}, K_{yx}, K_{yy}$: Oil-film stiffness coefficients

$\bar{K}_{xx}, \bar{K}_{xy}, \bar{K}_{yx}, \bar{K}_{yy}$: Dimensionless oil- film stiffness coefficients, $\bar{K}_{xx} = K_{xx}(c/W)$

L : bearing length

N : Journal rotational Speed

O_i : Lobe center of lobe i (i =1, 2, 3, 4)

p : Oil-film pressure

R : Journal radius

S : Sommerfeld no. $\frac{\mu NLD}{W}\left(\frac{R}{c}\right)^2$

V : Peripheral speed of journal

W : bearing external load

x, z : coordinates for bearing surface (x-peripheral, z-along shaft axis)

ϕ : Attitude angle

$\dot{\alpha}$: Whirl rate ratio, $\dot{\alpha} = \dot{\phi}/\omega$

$\dot{\beta}$: Squeeze rate ratio, $\dot{\beta} = \dot{\varepsilon}/\omega$

ε : Eccentricity ratio, e/c

δ : Ellipticity ratio, $(1 - c_m/c)$

θ : Angle measured from the line of centers in the direction of rotation

θ_g : Oil-groove angle

ρ : Fluid density

μ : Average fluid viscosity

ω : Rotational speed

ν : Dimensionless threshold speed, $\omega(c/g)^{1/2}$

References

1. Garner, D.R., Lee, C.S. and Martin, F.A. (1980) Stability of profile bore bearings, Influence of bearing type selection. Tribology International, pp. 204-210.
2. Hagg, A.C. (1946) The influence of oil film journal bearing on the stability of rotating machines. J. App. Mech., Trans. ASME, A-211.
3. Booke G.F. and Strenlitch, B. (1956) Investigation of translatory fluid whirl in vertical machines. Trans. ASME, p.13.
4. Nicholas J.C. and Allaire, P.E. (1980) Analysis of Step Journal Bearings- Finite Length Stability. ASLE Trans., pp. 197-207.
5. Li, D.F., Choy, K.C. and Allaire, P.E. (1980) Stability and Transient characteristics of four multilobe journal bearing configuration. TRANS ASME. Journal of Lubrication technology, pp. 291-299.
6. Nicholas, J.C. and Allaire, P.E. (1980) Stiffness and damping coefficients for finite length step journal bearings. ASLE Trans., pp. 353-362.
7. Mehta, N.P. and Singh, A. (1987). Stability of Finite Orthogonally-Displaced Pressure Dam Bearings. ASME Journal of Tribology, vol. 109, no. 4, pp. 718-720.
8. Flack, R.D., Leader M.E. and Gunter (1980) An Experimental Investigation on the Response of a Flexible Rotor Mounted in Pressure Dam Bearings, Trans. ASME. Journal of Mechanical Design, pp. 842-850.
9. Mehta N.P., Singh, A. and Gupta, B.K. (1986) Dynamic Analysis of Finite Half-Elliptical Pressure Dam Bearings with Rotor Flexibility Effects. ASLE Trans., vol. 29, no. 1, pp. 61-66.
10. Mehta N. P., Singh, A. and Gupta B. K. (1986). Stability of Finite Elliptical Pressure Dam Bearings with Rotor Flexibility Effects. ASLE Trans., vol.29, no. 4, pp. 548-557.
11. Mehta N. P., Rattan S. S. and Rajiv, V. (2010) Stability Analysis of Two Lobes Hydrodynamic Bearings With Couple Stress Lubricant. ARPN Journal of Eng. And Applied Sciences, no. 5, pp. 69-74,
12. Malik, M., Chandra, M. and Sinhasan, R. (1982) Design Data for Offset-Halves Journal Bearings in Laminar and Turbulent Flow Regimes. ASLE Trans., pp. 133-140.
13. Mehta N.P., Rattan S.S. and Gian, B. (2003) Static and Dynamic Characteristics of Four-Lobe Pressure Dam Bearings, Tribology Letters, vol. 15, no. 4, pp. 415-420.
14. Malik, R., Sinhasan and Chandra, M. (1981) A Comparative Study of Some Three-lobe Bearing Configurations. Wear, pp. 277-286.
15. Booker, G.F. and Hubner, K.H. (1972) Application of Finite Elements to Lubrication: An Engineering Approach. Trans ASME, Journal of Lubrication Technology, pp. 313-323.
16. Kumar, A., Sinhasan, R., and Singh, D. (1980) Performance characteristics of a two lobe hydrodynamic bearing. Trans. ASME, Journal of Lubrication Technology, pp. 425-429.
17. Mehta N.P., Rattan S.S. and Reddy (1990) Effect of preset on Static and Dynamic Characteristics of Orthogonally-Displaced Bearing. Proceedings of the international Tribology conference (Nagoya, Japan), pp. 1665-1670.
18. Booker, G.F. and Hubner, K.H. (1972) Application to finite elements to lubrication an engineering approach. Journal of Lubrication Technology, pp. 313-323.
19. McCallion H., Smalley A.J., Lloyd, T. and Harsnell, R. (1980) A Comparison of performance for Steadily Loaded Journal Bearings. Proc. Lubrication and Wear Conference (Institute of Mechanical Engineers, London), 180(12).
20. Booker J .F and Goenka, P.K. (1980) Spherical Bearings: Static and Dynamic Analysis via the Finite Element Method, Trans. ASME Journal of Lubrication Technology, pp. 308-319.
21. Pinkus, O. and Strenlitch, B. (1961) Theory of lubrication (McGraw-Hill, New York).